

Relative Phase Reconstruction Based on Multiprobe Solutions and Post-Processing Techniques

Rubén Tena Sánchez¹, Manuel Sierra Castañer¹, L.J. Foged²,

¹Centro de Investigación en Procesado de la Información y Telecomunicaciones, ETSI Telecomunicación Universidad Politécnica de Madrid 28040, Madrid, Spain, rubents93@gr.ssr.upm.es, manuel.sierra@upm.es

²MVG, Microwave Vision Group, Pomezia Rome, Italy, lars.foged@mvg-world.com

Abstract—In a previous paper a referenceless measurement set-up based on a reference antenna was used to characterize the near-field radiation of antennas in the planar and spherical multiprobe systems. This paper proposes an alternative technique based on exploiting the intrinsic characteristics of multiprobe systems. One of the antennas from the multiprobe arch is used to retrieve the relative phase between measurement points. Post-processing is needed since the relative phase between azimuth cuts is lost. The advantages, limitations and results are shown. The results demonstrate that the technique is very promising for characterizing devices under certain conditions.

Index Terms—phase difference, post-processing, multiprobe, antenna measurements.

I. INTRODUCTION

There is a clear demand of wireless communications, whether it is 5G, Zigbee, Wi-Fi or any other technology. This is leading to the necessity of integration of the devices, thus the antenna is part of the overall design of the system. The users can benefit from this integration, nevertheless there are also a lot of challenges from the designing point of view. The measurement of these devices is far from trivial, since the signal from the source is not accessible and therefore the phase can not be acquired. In other cases, it is not the fact that the signal is not accessible but the unintended radiation of the integrated device that needs to be measured.

Conventional near-field measurements can not deal with these scenarios. There is a wide range of amplitude only method solutions to retrieve the phase of the field. Holographic techniques [1] has been studied in the literature for the planar geometry. It requires further hardware to generate the reference field, and due to overlapping in the spectral domain it may require a high sampling rate. The two scans technique is also a possible solution, but the measurement time is increased and it is very sensitive to the initial guess and independence of the information obtained from both surfaces. Mean errors about -35 dB were achieved in [2] by choosing the proper initial guess and separation between acquisition planes. Interferometry methods [3] or probe with multiple outputs [4] have also been tested in the literature. The drawback of interferometry is the necessity of extra hardware to process the in-quadrature and in-phase combination of signals and the risk of propagated errors. The errors may be minimized by using linear combination of signals at different positions, but the measurement time is increased.

In [5], a time domain over the air (OTA) measurement set-up was introduced. A phase recovery unit that exploits the radiation of the device to get a reference signal by using a reference antenna was used. However, there are some limitations mainly attributed to the interference of the reference antenna, although post-processing techniques can minimize this perturbation. For the spherical multiprobe system, average errors below -38 dB were achieved for the measurement of a linear polarized standard gain horn at 2.3GHz.

In this paper a contribution to the problem of characterizing the relative phase between measurement probes is presented. The technique is based on using one of the antennas from the multiprobe arch. The solution proposed is in the middle way of the solutions proposed in [3], [5]. The difference with the last is that the linear combination of signals from different probes in-phase and in-quadrature is substituted by the relative phase calculated by using the top-probe from the arch as a reference. This solution present a clear advantage since the radiation of the device is not perturbed by a reference antenna. Nevertheless, there are some challenges to face, like the necessity of calibration and the unknown phase between different azimuth cuts.

The paper is organized as follows: in Section II an explanation of the multiprobe system and the phase retrieval algorithm is given. Section III will show a simulation example for linear polarization and will discuss some of the limitations and how to solve them in a real scenario. In Section IV the proposed technique is validated by measuring in a real multiprobe system. Finally, Section V will present the conclusions and future lines.

II. MULTIPROBE MEASUREMENT SYSTEM AND PHASE RETRIEVAL ALGORITHM

Spherical multi-probe measurement systems are near-field solutions designed to overcome high acquisition times that are present in single probe solutions [6]. The probe array consisted of a group of evenly spaced dual polarized elements along a circumference. The measurements are performed by electrically commuting between different outputs of a combiner network. The whole sphere is sampled by rotating the device under test (DUT) in azimuth. The array can also rotate around its center and increase the sampling rate by the widely known over-sampling factor. If passive measurements are performed, the vector network analyzer (VNA) is connected to the DUT

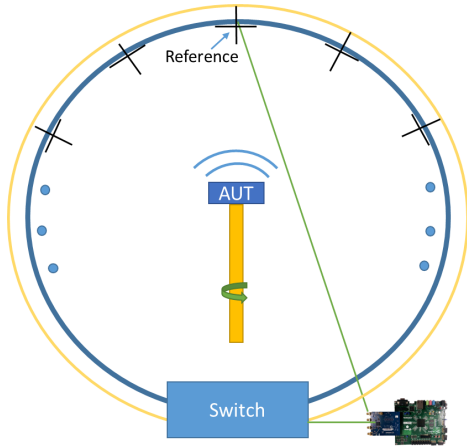


Fig. 1. Measurement set-up

and output of the combiner network. In this work, a low-cost alternative based on the substitution of the VNA for a software defined radio (SDR) receiver is implemented. The use of a low-cost receiver is suitable for saving time and resources in scenarios like electromagnetic compatibility (EMC).

The geometry of the problem can be seen in Fig. 1. The top-probe of the measurement arch is going to be the reference to retrieve the relative phase between sampling points. The top probe will measure the projection of the electromagnetic field into different directions when the DUT is rotating along its axis. Therefore, the relative phase between cuts may be reconstructed if the polarization properties of the field are calculated. For the sake of simplicity non-oversampling scenarios will be considered in the following derivation. Lets assume that the even number N represents the probes that compose the multiprobe system (the analogous would be done for an odd number). Depending on the multiprobe system, the azimuth range must go up to 180° or 360° . Then, if equi-sampling in elevation and azimuth is assumed, the number of azimuth cuts needed will be equal to $2N-2$ (full range in azimuth) or $N/2$ (full range in elevation). When a measurement is performed, the system is considered stationary for every azimuth cut. The last means that the relative phase between probes of the same cut is retrieved properly under ideal conditions. If full range in azimuth is assumed, Eq. (1) represents the unknown phase terms involved in the retrieval process:

$$\begin{aligned}
 \vec{E}_{meas}(S_1) &= \vec{E}_{ref} \\
 \vec{E}_{meas}(S_2) &= \vec{E}(S_2)e^{j\phi_2} \\
 &\vdots \\
 \vec{E}_{meas}(S_{2N-2}) &= \vec{E}(S_{2N-2})e^{j\phi_{2N-2}}
 \end{aligned} \tag{1}$$

In the last equation, $\vec{E}_{meas}(S_i)$ represents the sampled electric field for each i acquisition in azimuth, whereas $\vec{E}(S_i)$ is the ideal field. The exponential term accounts for phase shifts introduced for each cut due to the rotation of the top probe. One way of retrieving the lost phase reference is by appealing to Ludwig's third definition of polarization for the top probe

[7]. The definition projects the measurements always into a vector that has the same direction. Eq. (2) describes the directional vectors used for the projection of the measured electromagnetic field.

$$\begin{aligned}
 \hat{\mathbf{E}}_{\text{CP}} &= \hat{\theta} \cos(\phi - \phi_0) - \hat{\phi} \sin(\phi - \phi_0) \\
 \hat{\mathbf{E}}_{\text{XP}} &= \hat{\theta} \sin(\phi - \phi_0) + \hat{\phi} \cos(\phi - \phi_0)
 \end{aligned} \tag{2}$$

Therefore, the phase error will be projected into Ludwig's vectors and by comparing the retrieve phase for each cut with respect to a reference cut, the relative phases can be reconstructed. The term ϕ_0 of Eq. (2) will be critical depending on the received polarization, since to ensure certain level of uncertainty it is necessary to estimate the phase error of the Ludwig's vectors with enough accuracy. To do that, the tilt angle with respect to θ -axis can be retrieved as described by Eq. (3), where δ is the relative phase between E_θ and E_ϕ components of the field and τ is the well known tilt-angle of the polarization ellipse.

$$\begin{aligned}
 \delta &= \phi_\theta - \phi_\phi \\
 \tau &= \frac{1}{2} \text{atan}\left(\frac{2|E_\theta||E_\phi|}{|E_\theta|^2 - |E_\phi|^2} \cos(\delta)\right)
 \end{aligned} \tag{3}$$

If the tilt angle is calculated, then the term ϕ_0 can be computed for different cuts and the average value will give the direction of the major axis of the polarization ellipse that should be parallel to the direction of the Ludwig's vectors. In this way, the fields with the largest signal to noise ratio (SNR) are weighted properly and the errors are minimized.

III. SIMULATED PHASE RETRIEVAL CAPABILITIES

From the previous considerations it is clear that the numerical performance of the algorithm will depend on the SNR on the top-probe and the purity of the measured polarization ellipse (amplitude and phase errors introduced by the measurement system). For the following simulations, only errors due to the low-cost receiver will be considered, and the system will be considered ideal. The results will provide a good insight of the best results and limitations that will be found in the system due to the receiver and SNR on the top probe. The errors introduced in the real system will be evaluated by testing measured data in Section IV.

The low-cost receiver is the same as the one used in [5]. The empirical noise statistics of the receiver were characterized and compared with a simulated signal model demonstrating the good correlation between the model and the measurements. Thereby, the signal model will be used to introduce errors in amplitude and phase depending on the SNR of the sampled probe and reference top probe.

The following simulations consider that each measurement sample is contaminated with noise as described in Eq. (4); X_ϕ and $X_{|A|}$ refers to Gaussian distributions with 0 mean and standard deviation equal to 1. The standard deviations $\sigma_{|A|}$ and σ_ϕ account for the uncertainties depending on the SNR of the top-probe (reference) and measurement probe. Thus, the phase of the top-probe is considered zero and only amplitude errors are introduced in this probe for different azimuth cuts.

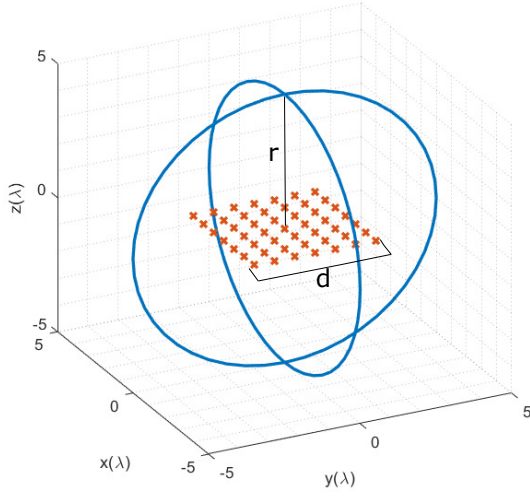


Fig. 2. Simulated acquisition for numerical validation

$$\vec{E}_{sim} = (|E_{sim}| + \sigma_{|A|} \cdot X_{|A|}) e^{j(\phi + \sigma_{\phi} \cdot X_{\phi})} \quad (4)$$

The errors introduced by the reference top-probe can be analyzed without simulating electrically large problems. Therefore, the effect of the noise introduced by the low-cost receiver and the top probe reference channel will be analyzed for electrically small problems for the sake of simulation time. Without loss of generality, the simulation consists of a square array of Hertzian dipoles along the xy -plane, see Fig. 2. The square array side "d" is 2λ and the measurement radius "r" 5λ . Considering Eq. (5), the $\Delta\theta$ and $\Delta\phi$ steps are 7.5° . The simulations are done by considering full range in ϕ , and θ going from 0° to 180° .

$$N = kr + 10 \quad (5)$$

The worst case scenario will be faced for linear polarization. The reference channel will be connected to one polarization of the top probes. This will be translated into large phase errors for ϕ cuts where the energy is projected into the orthogonal polarization.

If the Hertzian dipoles are linear polarized in the x -direction and the θ -component of the field is considered as the reference the phase errors after reconstructing the phase will be concentrated around $\phi=90^\circ$ and $\phi=270^\circ$, see Fig. 3. In the figure, the error is computed as described in Eq. (6) by comparing the reference simulated field with the reconstructed one by using Ludwig's projections and choosing the proper value of τ . The mean error for E_θ and E_ϕ components is -68dB and -65dB respectively. That is reasonable since the dynamic range of the SDR is about 60dB .

$$\epsilon \text{ (dB)} = 20 \log_{10} |\vec{E}_{ref} - \vec{E}_{reconstructed}| \quad (6)$$

However, the phase errors introduced for E_ϕ at $\phi=90^\circ$ and $\phi=270^\circ$ are very high. These errors will be translated into the

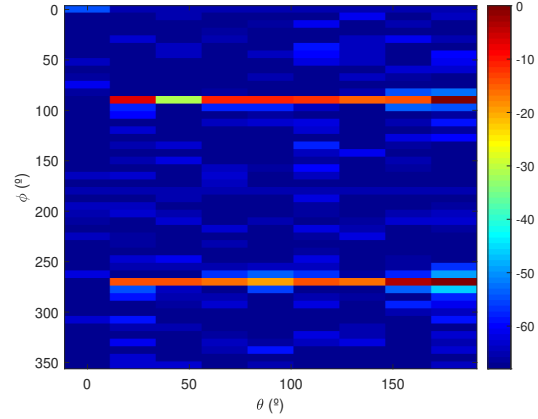


Fig. 3. Near-field error for E_ϕ

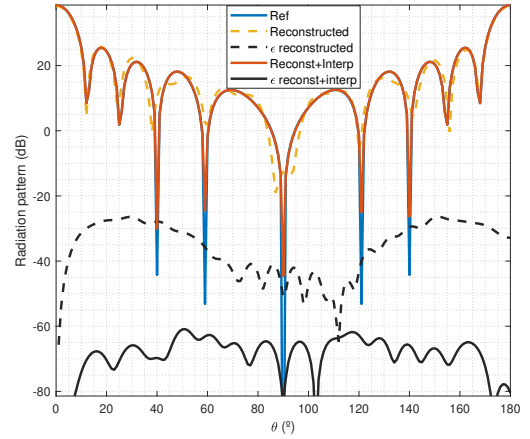


Fig. 4. Far-field error for E_θ , $\phi = 0^\circ$

modal expansion and will be propagated to the far-field, thus, worsen the performance of the pattern estimation. When the field is sampled properly, the amplitude of the cuts could be maintained and phase interpolation. If this is done, the errors are minimized, since the phase errors are minimized and so the errors in the modal expansion.

The error analysis for the main cuts of the radiation pattern in the far-field before and after applying the interpolation can be seen in Figs. 4 and 5.

The good performance obtained by using interpolation in the simulations is subject to the step needed in ϕ since the smaller the step the closer the field will be to asymptote that makes the reference signal tends to zero for ideal linear polarization. Nevertheless, in a real scenario, the signal transmitted in the orthogonal polarization will not be zero, and therefore this problem just represents a worst case but not a real measurement. In fact, even misalignment errors will help to mitigate this error. Thereby, the level of the signal at the reference top probe of the surrounding cuts will determine the level of uncertainty of the interpolated cut. Levels around -30dB below

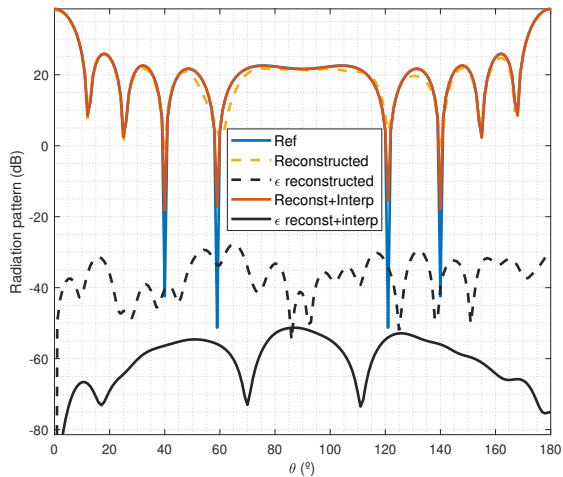


Fig. 5. Far-field error for E_ϕ , $\phi = 90^\circ$

the maximum of the major axis of the polarization ellipse should be enough to provide low errors when calculating the modal expansion. Otherwise, interpolation or other practical approaches should be applied, like choosing a ϕ grid that avoids the cuts with minimum power by maintaining the required sampling step.

If circular polarization is used very low errors are expected, since the SNR on the top probe when rotating in azimuth does not decrease. The intermediate performance of the post-processing algorithm is expected for a general elliptical polarization. To summarize, the following challenges and solutions will define the accuracy of the phase reconstruction if the system is considered ideal and only errors due to the receiver are considered:

- Low SNR on the top probe. It can be compensated by using the SDR receiver gain, that goes up to 60dB.
- Radiated polarization that tends to linear. Interpolation, modal filtering or defining a new ϕ grid will help to resolve this problem.

IV. MEASUREMENT SET-UP AND RESULTS

The previous analysis showed the potential of the technique in order to reconstruct the radiated phase of a DUT by using the top probe of a multiprobe system as a reference. The main limitations of the system due to the receiver and reference channel were analyzed and a simulated example was presented. Finally, a measurement set-up based on the OTA test system MiniLab from Satimo will be presented.

The radiation pattern of a standard gain horn antenna (SGH2000) will be measured by the VNA and the proposed technique. The antenna will be measured at 1GHz so that oversampling is not needed in the MiniLab. In Fig. 6, the measurement set-up can be seen. The antenna is slightly offset with respect to the z -axis due to the interface. Nevertheless, the two measurements will be done by using the same set-up, thus the comparison between patterns can be performed without introducing errors due to the positioning.

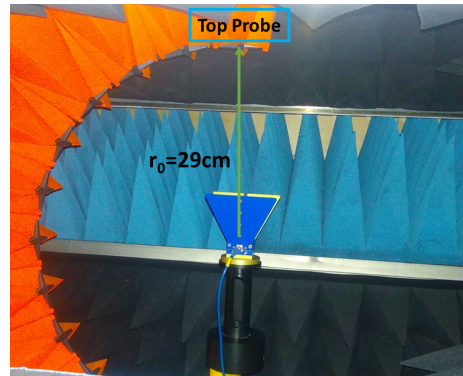


Fig. 6. MiniLab measurement set-up

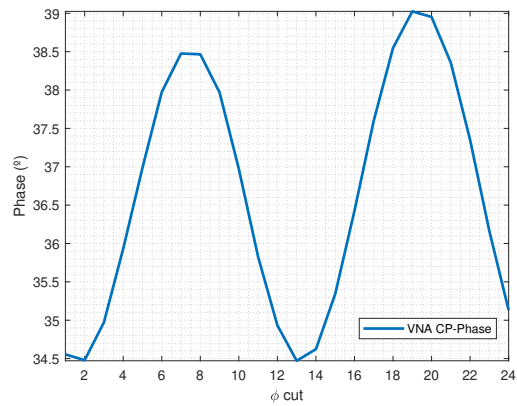


Fig. 7. Copolar phase on the top-probe for VNA measurement

A. Calibration

In [5] the calibration step was not necessary since the reference antenna was not part of the measurement system. If the top-probe antenna is the reference, it is mandatory to calibrate the SDR ports and the path differences between the probes and the top-probe. Once it is done, the amplitude and phase calibration coefficients are applied to the measurement of the top-probe and the phase reconstruction can be implemented.

It is important to remark that probe calibration is also very important if the aim is to minimize the phase reconstruction error. To illustrate this, let's analyze the phase of the copolar component according to Ludwig's third definition of the measurement of the SGH2000 by using the VNA, see Fig. 7.

The last figure represent the errors introduced in the copolar vector due to inaccuracy in the probe correction. Since this is the case, the problem to be solved is represented by Eq. (7), where n is a complex noise term and ϵ is a complex term that accounts for amplitude and phase errors due to calibration.

$$\begin{aligned} \vec{\mathbf{E}}_{\theta\epsilon} &= \vec{\mathbf{E}}_{\theta} + n + \epsilon_{cal} \\ \vec{\mathbf{E}}_{\phi\epsilon} &= \vec{\mathbf{E}}_{\phi} + n + \epsilon_{cal} \end{aligned} \quad (7)$$

When forcing the copolar vector to have the same phase for every ϕ cut at the top-probe, an error will be introduced

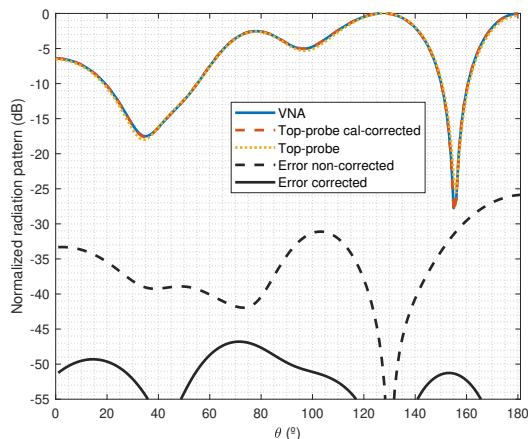


Fig. 8. Copolar far-field radiation pattern of SGH2000, $\phi = 0^\circ$

with respect to the VNA measurements. This error can not be neglected and only a proper calibration will remove the uncertainty of phase errors introduced in E_θ and E_ϕ . To confirm that the calibration will reduce drastically the errors introduced, the phase error of the copolar vector of the VNA measurements was used to correct the retrieved phase by the top-probe technique. In order to do that the retrieved copolar was multiplied by the difference between the known copolar phase from the VNA measurement and the extracted one.

B. Measurement results

The measurement results showed the effect of the calibration errors. Moreover, between the VNA and top-probe technique measurements the errors are worse because the interface was not completely stable and it was necessary to move the MiniLab between measurements to access the top-probe, thus, introducing uncertainties between measurements. In Figs. 8 and 9, the far-field radiation pattern and the error can be observed. Despite the challenges described for the measurement set-up the retrieved far-field is in good agreement with the VNA measurements. The corrected results should be interpreted as the results that could be obtained if the calibration is performed carefully. In particular, the average near-field errors of the measured points are improved from -38dB to -48.2dB for E_θ and from -37dB to -47.9dB for E_ϕ . Therefore if the calibration is applied properly the error could be as good as these post-processed results.

V. CONCLUSION AND FUTURE LINES

The development of a low-cost multiprobe OTA measurement system based on reconstructing the phase by using the top-probe has been presented. First, some simulations has been presented to show some of the limitations of the system. Linear polarization or antennas with poor radiation towards the top probe are the worst scenarios. Nevertheless, in a practical measurement linear polarization will not be that critical. For energy de-pointing from the broadside direction, the gain of the receiver can be used to compensate in terms of SNR.

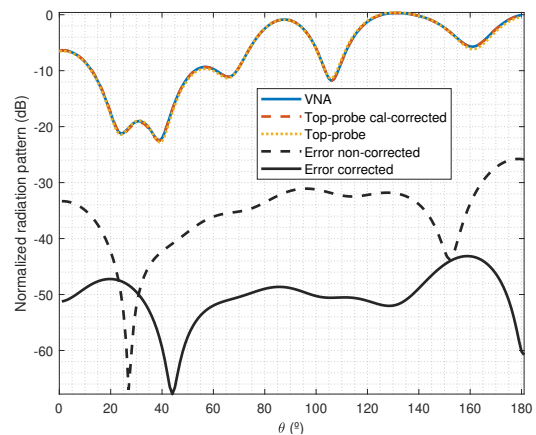


Fig. 9. Crosspolar far-field radiation pattern of SGH2000, $\phi = 0^\circ$

The performance of the algorithm is strongly dependent on the accuracy of the calibration coefficients. The effects of this calibration has been presented and the ideal results that could be expected if a good calibration is used has been estimated by applying a correction factor. The good results demonstrate the potential of the technique. Oversampling scenarios and more challenging radiation patterns are under research.

ACKNOWLEDGEMENT

Authors would like to acknowledge the Spanish Government, Ministry of Economy, National Program of Research, Development and Innovation for the support of this publication in the project FUTURE-RADIO "Radio systems and technologies for high capacity terrestrial and satellite communications in an hyperconnected world" (project number TEC2017-85529-C3-1-R). Francesco Saccardi and Alessandro Scannavini are acknowledged for their help during the measurements.

REFERENCES

- [1] A. Arboleya, J. Laviada, J. Ala-Laurinaho, Y. Álvarez, F. Las-heras, and A. V. Räsänen, "Reduced set of points in phaseless broadband near-field antenna measurement : Effects of noise and mechanical errors," *2016 10th European Conference on Antennas and Propagation (EuCAP)*, Davos, pp. 1–5, 2016.
- [2] J. F. Alvarez and O. Breinbjerg, "Towards Planar Phaseless Near-Field Measurements of ESA's JUICE Mission 600 GHz SWI Reflector Antenna," *AMTA 2016 Proceedings*, pp. 1–6, 2016.
- [3] A. Paulus, J. Knapp, and T. F. Eibert, "Utilizing partial knowledge of phase differences in convex optimization for amplitude-only near-field far-field transformation," *2017 11th European Conference on Antennas and Propagation, EUCAP 2017*, pp. 3766–3770, 2017.
- [4] M. Spang, T. Stoeckel, G. Schubert, and M. Albach, "Application of probes with multiple outputs on probe-compensated EMC near-field measurements," *2010 IEEE International Conference on Industrial Technology, Vina del Mar*, pp. 188–193, 2010.
- [5] R. Tena Sanchez and M. S. Castaner, "Evaluation of software defined radio receiver for phaseless near-field measurements," *2018 AMTA Proceedings, Williamsburg*, pp. 1–6, 2018.
- [6] L. J. Foged and A. Scannavini, "Efficient testing of wireless devices from 800 MHz to 18 GHz," *Radioengineering*, pp. 460–466, 2009.
- [7] A. C. Ludwig, "The Definition of Cross Polarization," *IEEE Trans. on Ant. and Prop.*, vol. Vol. AP-21, no. No. 1, pp. 116 – 119, 1973.